Computers and Chemical Engineering 194 (2025) 108978

Contents lists available at ScienceDirect

Computers and Chemical Engineering

journal homepage: www.elsevier.com/locate/compchemeng

Simple control structure for stabilizing Core Annular Flow operation in heavy oil transportation

Patrick Lima [a], Erbet Costa [a], Teófilo Paiva Guimarães Mendes [b], Leizer Schnitman [b], Sigurd Skogestad [a,*], Idelfonso Nogueira [a,*]

[a] Department of Chemical Engineering, Norwegian University of Science and Technology (NTNU), 7491 Trondheim, Norway
[b] Programa de Pós-Graduação em Mecatrônica, Federal University of Bahia, Rua Prof. Aristides Novis, 2, Federação, Salvador 40210-630, Brazil

ARTICLE INFO

Keywords:
Core Annular Flow
Computational fluid dynamics
PI controller
Multiphase flow

ABSTRACT

This research aims to develop a simple regulatory controller to control a Core Annular Flow (CAF) in the oil and gas industry, focusing on transporting heavy oils. CAF is an economical method to transport viscous crude oil where less viscous liquid, typically water, is used to lubricate the pipe walls, creating an annular flow regime. However, managing the stability of CAF is challenging due to geometric variations, changes in pipeline flow direction, and emulsion formation. We used computational fluid dynamics (CFD) simulations to represent the CAF system and subsequently designed a simple control structure for the process. This process involved conducting both open-loop and closed-loop tests. The findings from the study indicate that the I controller significantly improves the system's response to disturbances in oil velocity by adeptly adjusting water velocity. This adjustment is crucial for maintaining the desired oil fraction and sustaining an annular flow pattern. An important observation was the effectiveness of the proportional gain in tracking the setpoint within annular flow regimes and the enhanced system stability achieved by increasing the integral action. The study concludes that the PI controller stabilizes operations in previously challenging conditions and expands the system's operational range.

1. Introduction

The Core Annular Flow (CAF) pattern is a critical fluid dynamics phenomenon in multiphase flow systems, wherein a high-viscosity fluid, such as heavy crude oil, is encircled by a less viscous fluid, forming an external annular layer within pipelines. In many industrial applications, water serves as the external fluid, functioning as a lubricating layer around the core of viscous oil. This configuration is paramount in sectors like the oil and gas industry (Joseph et al., 1997), where it aids in minimizing frictional resistance between the oil and the pipeline, optimizing flow efficiency, and reducing energy consumption (Tripathi et al., 2017).

A visual representation of this system, as shown in Figs. 1a and Fig. 1b, depicts high-viscosity oil in red at the center of the flow surrounded by water in blue, functioning as a lubricating layer. This arrangement improves fluid transportation efficiency and reduces pumping costs and environmental impact. As you can observe in Figs. 1a and Fig. 1b, the interface between water and oil for the CAF operation exhibits a wavy behavior, indicating proximity to instability. This delicate balance means that any disturbances in the system could lead to a regime transition, placing the process in an unstable and suboptimal operating regime.

This system is widely used in large-scale industrial applications. For example, a 55 km Orimulsion pipeline in Venezuela has successfully operated with CAF between Sandiego, Anzoategui, and the Budaré treatment station. Shell utilized a CAF installation in California for 12 years, pumping oil water through a 38.6 km pipeline with a 24,000 barrels per day flow rate (Salager et al., 2010). The pressure loss in the latter project ranged from 900 to 1100 psi (Bensakhria et al., 2004).

Although widely employed in large-scale transport systems, CAF encounters several challenges that require careful consideration. These challenges encompass the destabilization of annular flow due to geometric variations or alterations in the pipeline's flow direction, fouling caused by viscous fluids adhering to the pipeline wall, and emulsion formation resulting from solid impurities or water present in the fluid, which may compromise the stability of the annular flow pattern (Rosa,

* Corresponding authors.
E-mail addresses: sigurd.skogestad@ntnu.no (S. Skogestad), idelfonso.b.d.r.nogueira@ntnu.no (I. Nogueira).

https://doi.org/10.1016/j.compchemeng.2024.108978
Received 29 May 2024; Received in revised form 10 November 2024; Accepted 9 December 2024
Available online 12 December 2024

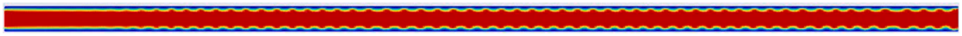

Fig. 1a. Example of Core Annular Flow, side view.

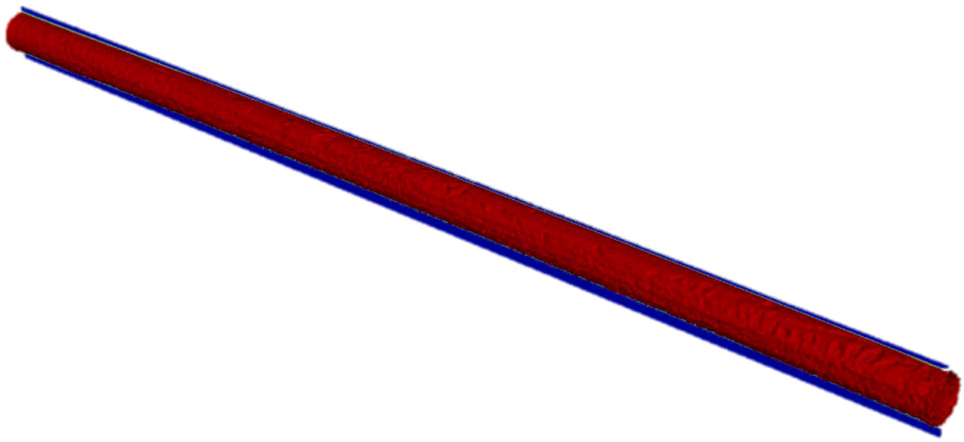

Fig. 1b. Example of Core Annular Flow, isometric view.

2012). Ensuring the stability of CAF, especially over extended distances, presents additional complexities, largely attributed to the buoyancy effect. Addressing these obstacles is crucial for optimizing the efficiency and effectiveness of CAF applications across various industries (Joseph et al., 1997; Bensakhria et al., 2004). Given this, the introduction of control structures becomes an important contribution. Remarkably, PI controllers, known for their stabilizing properties, have not traditionally been employed in CAF systems. Moreover, the employment of simple control structures for flow stabilization is not usually seen in the literature. This can potentially be a promising solution to overcome these obstacles and enhance the overall performance of oil and gas transport processes.

Salager et al. (2010), Versteeg and Malalasekera (2007), and Storkaas (2005, 2007) alongside Sivertsen and Storkaas (2010) have highlighted the challenges and opportunities in controlling fluid flow regimes within pipelines, which is still a valuable but usually neglected area for control engineers due to the potential for improved operation through technology. In the referred works, the authors point out that traditional methods for analyzing pipeline flow have been based on the flow regimes that develop under different boundary conditions. However, by employing feedback control, it is possible to enhance the stability of these flow regimes. Specifically, the mentioned papers cite the transition from laminar to turbulent flow in single-phase pipelines at a certain Reynolds number. Although higher Reynolds numbers have been found to have unstable laminar flow regions, the document suggests that stabilization of the laminar flow should theoretically be feasible. Despite this, such control applications present no practical application, and the referred works cover unstable flow phenomena in multiphase pipelines, such as slug flow, which velocity differences between gas and liquid phases or pipeline geometry can cause (Storkaas, 2005; Storkaas, 2005; Storkaas, 2007; Sivertsen and Storkaas, 2010; Storkaas, 2002).

Even though we did not find any existing literature explicitly focusing on control approaches within CAF systems, simple regulatory control structures have significant applications in tackling challenges related to oil and gas transport, as documented in the works referred to above and by (Jahanshahi et al., 2012). In this research, the authors sought to devise a straightforward and resilient control structure to stabilize gas-lifted oil wells and prevent casing-heading instability. They conducted a controllability analysis using a range of potential control variables and manipulated variables, ultimately establishing an effective control structure based on top-side pressure measurements.

In a subsequent study by (Jahanshahi and Skogestad, 2013), PI and PID controllers were utilized to avert unstable flow in offshore oil fields. The researchers suggested robust and practical tuning rules through model identification and IMC design, corroborating their findings using test rigs and simulations with the OLGA simulator.

In this scenario, CFD is a useful tool for understanding and providing insights into CAF systems' fluid dynamics and interactions. Furthermore, a rigorous CFD simulation can be used as a development platform for control strategies to address the above stability issues. CFD simulations have been used in the CAF literature for other applications. For instance, Ghosh et al. (2010) used CFD to simulate core-annular downflow in vertical pipes for energy-efficient water-lubricated transport of highly viscous oil. Utilizing Ansys Fluent, the results match experimental data satisfactorily and provide detailed profiles of key parameters across various inlet velocities (Ghosh et al., 2010).

Jiang et al. (2014) employed a CFD Eulerian model to simulate oil-water core annular flow in a U-bend, comparing results with experimental data and the volume-of-fluid (VOF) model. Findings inform optimal U-bend pipefitting design (Jiang et al., 2014).

Xie et al. (2023) provided a comprehensive review of the energy-saving aspects of CAF in heavy oil transportation, highlighting its economic and practical benefits in modern industrial applications. Their work underscores the ongoing research efforts to optimize CAF for more efficient and sustainable oil transport.

Dianita et al. (2021) explored the complexities of CAF in oil-water systems, particularly focusing on the effects of pipeline junctions (T- and Y-junctions) on flow stability and efficiency using computational fluid dynamics and statistical experimental design. This research highlights the continuous advancements in understanding and modeling CAF in complex pipeline networks, which is crucial for optimizing industrial processes.

Inspired by these principles, this work addresses the challenges associated with regime transition in multiphase liquid flow. It might be possible to control annular flow stability over long distances using simple control structures based on virtual plant for CAF dynamic studies with CFD rigorous simulations. This might be possible to do with the flow rates as manipulated variables and using a given system property that can give feedback to the control system on the information related to the flow stability. This might result in a more reliable and efficient transport solution for industries utilizing CAF systems.

Therefore, this paper aims to propose and validate control strategies applied to a CAF system simulated by Computational Fluid Dynamics (CFD) methods. The controller's objective is to regulate the process in a

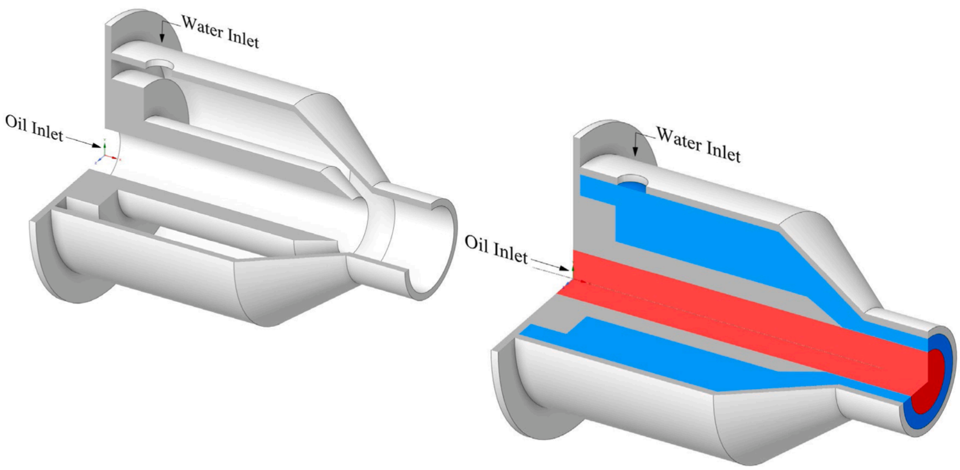

Fig. 2. Example of Core Annular Flow.

Fig. 3. Geometry of inlet system.

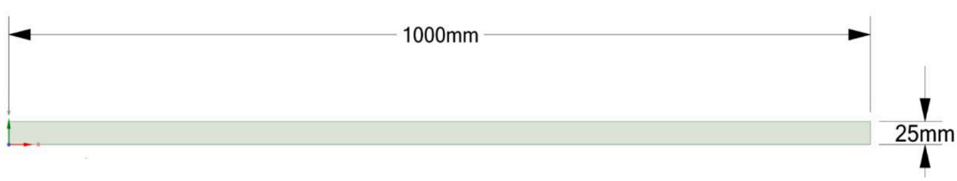

Fig. 4. System dimensions.

highly productive zone by increasing the spatial occupation of oil in the pipe's cross-section while avoiding fouling in unstable operation. The study explores the simple internal model control PID (SIMC-PID) method rules (Skogestad, 2003), which resulted in closed loop system robust to fluid dynamics disturbances.

2. CFD modelling and simulation

2.1. CASE study and virtual plant

The nozzle design is pivotal in the Core Annular Flow (CAF) system, particularly when transporting heavy and viscous crude oils. Its primary function is to facilitate the formation of a stable crude oil core encased in a surrounding annular layer of a less viscous fluid, typically water.

Typically, the nozzle will have a coaxial design comprising two concentric passages, Fig. 2. The inner passage allows the high-viscosity oil to flow, while the outer passage injects the less viscous fluid at a similar velocity. This design is critical to align the velocities of the two fluids, reducing shear forces at the interface and encouraging the formation of a lubricating film around the oil core.

Geometry development is the foundational step in CFD modeling, where a virtual representation of the physical domain is created. This representation must be precise and reflect the physical space in which the fluid flow will be studied. It includes the flow domain and integrates relevant geometrical features such as inlets, outlets, and physical obstructions. The quality of the geometry directly affects the subsequent mesh generation and overall solution accuracy, so advanced CAD software was used to ensure the geometry was as realistic as possible.

Fig. 3 presents the CAF inlet consisting of three entries representing the induction head: one 20 mm for oil and two 2.5 mm for water. The geometry of the CAF unit modelled is illustrated in Fig. 3.

This inlet was connected to a pipe, a straight, horizontal aluminum geometry with a length of 1000 mm, and a 25 mm diameter outlet was developed, as shown in Fig. 4.

Despite the laboratory-scale simulation of the geometry presenting some limitations, such as not fully capturing the behavior of core annular flow (CAF) during inclinations, curves, and variations in diameter, the chosen geometry is sufficiently robust for representing the flow pattern in a straight section of the pipeline. This makes it a reasonable choice for the case study we conducted.

The straight section allows us to focus on the fundamental dynamics of CAF without the added complexity of bends or varying diameters, which would significantly increase computational demands. While real-world pipelines do feature such complexities, the straight-section model provides a clear and controlled environment to study the core principles of CAF. This approach ensures that our findings are both relevant and applicable to real-world scenarios, particularly in sections of pipelines that are relatively straight and uniform.

After developing the geometry for our study, the domain needed to be systematically discretized into smaller units termed cells or elements,

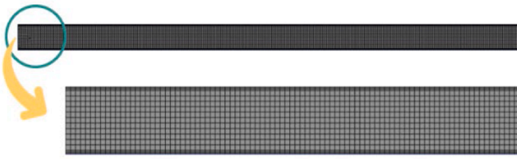

Number of nodes	Number of elements	Average of element quality
9033	8515	0.84

Fig. 5. Mesh of system.

Table 1
Physical chemist properties of system.

	Water	Oil
Specific Mass	$998.2\ \frac{kg}{m^3}$	$854\ \frac{kg}{m^3}$
Dynamic Viscosity	$0.001\ Pa\ s$	$0.62\ Pa\ s$
Interfacial Tension	$0.032\ \frac{N}{m}$	

a process known as mesh generation. This mesh is a foundational structure for conducting simulations, serving as a grid where the equations governing fluid dynamics are computed. Each cell in this mesh symbolizes a distinct segment of the overall domain, with the accuracy of the CFD simulation being intrinsically linked to the mesh's integrity. A more refined mesh enhances the detail in flow representation but concurrently escalates the computational demand and the time required for solution processing.

Carefully considering mesh resolution against the available computational resources is crucial to strike an optimal balance. Targeted mesh refinement is employed in areas necessitating heightened accuracy, for instance, near wall boundaries or in zones exhibiting significant gradients in flow properties. This specific study established the mesh configuration through a sensitivity analysis tailored to the intended application. Our goal is to create a virtual plant equipped with the proposed control structures; therefore, the mesh must deliver precise data and maintain a computational load that permits real-time analysis by the control systems. This balance ensures that the mesh is both informative and feasible for dynamic evaluations in a control-oriented environment.

A structured mesh was designed, featuring additional refinement layers near the wall boundaries. This design choice by sensitivity analysis culminated in forming a mesh comprising 9033 elements and 8515 nodes, ensuring comprehensive domain coverage. The quality of these elements was rigorously assessed, yielding an average quality score of approximately 0.84. This metric reflects the mesh's effectiveness in capturing the necessary flow details and underscores the balance achieved between precision and computational efficiency. The visual representation and detailed layout of this structured mesh are depicted in Fig. 5, illustrating the mesh and the strategic placement of refinement layers.

With the geometry set and mesh generated, the next step is setup configuration. This involves specifying the boundary conditions, which dictate how the fluid can enter, leave, or interact with the domain boundaries. The physical models are selected to match the physics of the problem. Governing equations, such as the Navier-Stokes equations for fluid motion, are defined during this step. Moreover, the physicochemical characteristics of the system, Table 1, were found in the literature of Jiang et al. (2014).

The interfacial tension, viscosity, and density are crucial properties in CFD modeling of multiphase flows. Interfacial tension determines the stability and morphology of the interfaces between phases. Viscosity influences the resistance to flow, while density affects the buoyancy and distribution of phases. Together, these properties are essential in accurately predicting flow dynamics (Rosa, 2012).

The gravity in the simulation was considered $9.81\ \frac{m}{s^2}$. This acceleration is important because there is a significant difference between the specific mass of oil and water, so the effect of buoyancy is relevant in the flow time.

Another crucial aspect of the setup is selecting the turbulence model, which is necessary for flows where turbulence plays a significant role. The choice of turbulence model ranging from simple models like Spalart-Allmaras to more complex ones like the Reynolds-Averaged Navier-Stokes (RANS) equations can greatly impact the simulation results. The selected model should match the flow characteristics and is vital for accurately capturing the turbulence's effects on the fluid flow.

Our study are primarily focuses on liquid-liquid flows, such as water-oil systems, where the rheological differences between liquid-liquid and liquid-gas systems are critical. As highlighted by Erni et al. (2004), the rheology at liquid-liquid interfaces differs significantly from liquid-gas systems, with smoother and less abrupt interface perturbations due to the lower density contrast and higher viscosity of the involved phases. This smoother interface reduces the need for complex turbulence models to capture intense dynamic interactions, making standard turbulence models like k-ϵ highly effective in such scenarios.

The k- ϵ model is widely recognized for its robustness, computational efficiency, and ability to provide a reliable approximation for a broad range of engineering problems, including multiphase flows. According to the ANSYS Fluent Theory Guide (ANSYS Inc, 2009), this model is well-suited for situations where interface perturbations are less severe, such as in liquid-liquid systems, allowing for effective flow representation without the need for more computationally intensive models.

Utilizing the RANS viscosity model with the standard K-epsilon and enhanced wall treatment in multiphase flow simulations strikes a balance between capturing complex turbulence-phase interactions and maintaining computational efficiency. This model is particularly adept at predicting near-wall effects crucial for phase behavior, such as coalescence, breakup, and deposition, without the computational burden of more detailed models like LES (Large Eddy Scales). The enhanced wall treatment improves accuracy in critical areas where phases interact with boundaries, essential for processes influenced by wall phenomena. Additionally, the standard K-epsilon model's widespread use provides a solid foundation to refine simulations. Its applicability across various multiphase scenarios, from droplet dispersion to sediment transport, makes it a versatile tool for engineering analyses.

The multiphase flow model adopted was the Volume of Fluid (VOF), which considers two Eulerian phases. The VOF is solved explicitly, with a Volume Fraction Cutoff of 1×10^{-6}. The interface model is of the Sharp type, and Brackbill et al. (1992) wall adhesion model is employed. The surface tension model also comes from Brackbill et al. (1992), with constant interfacial tension considered.

2.2. Simulations

Initiating with the CAF induction head concept described presented in Fig. 2, CFD simulations were performed using Ansys Fluent 2022 software, using the parameters and configuration described in Section 2.1. An isothermal system was considered, with the physicochemical data for the simulated fluids described in Table 1. The simulation was conducted in two dimensions. The physicochemical properties of the fluids are constant during the simulation. Ansys Space Claim 2022 R2 was used for the system's geometry construction. Ansys Meshing 2022

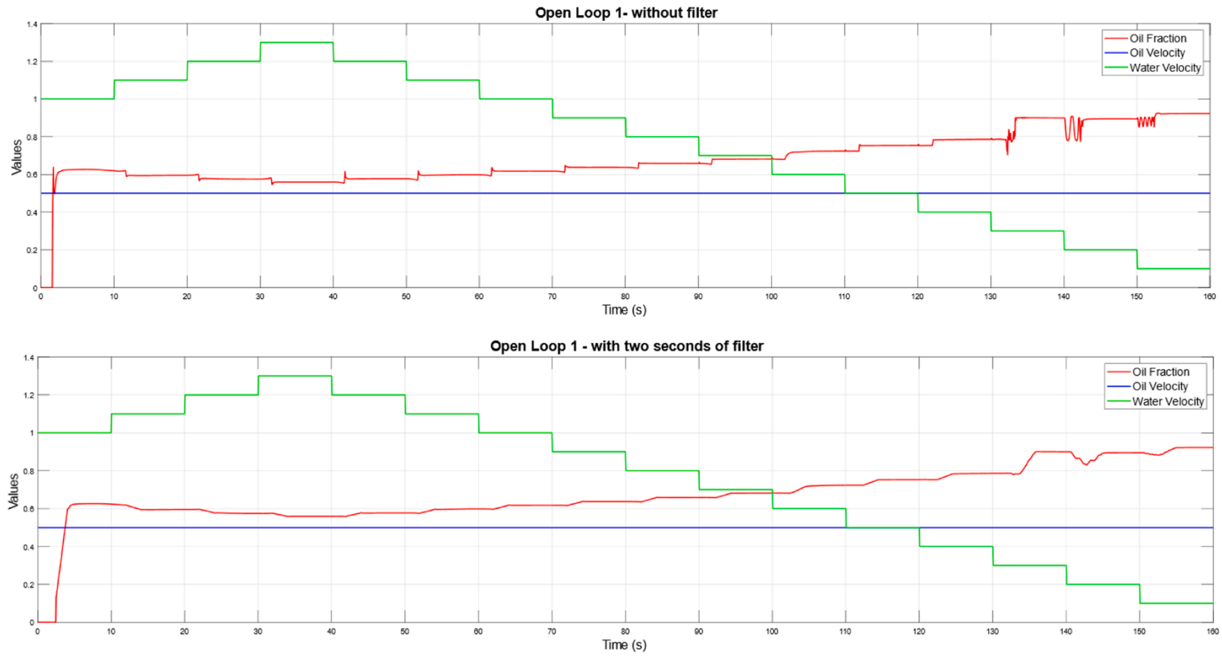

Fig. 6a. Open loop for oil velocity 0.5 m/s.

R2 was used to construct the system mesh.

After setting the configurations and initial conditions, the simulation is executed, and the software solves the governing equations in the discretized domain. Throughout the simulation, the convergence of solutions is monitored to ensure numerical stability.

Once the model proved to represent the expected behavior variations in CAF, a script was developed for the communication between Ansys, the simulator, and Matlab, the software used to implement the control. During the simulation using Ansys, the software was programed to generate a notepad in format .txt, for each iteration one line was written with oil fraction and the experiment time. After that, the notepad was read by Matlab where considering the sign value the action of control is taken. Once the new value of the manipulated variable is calculated, another notepad is generated with this value, which will be read by Ansys, thus starting another step simulation and closing the loop. This action can be done as many times as necessary. The calculations were done using one computer with 10 cores of 2.4 GHz.

Two open-loop tests were undertaken to understand the CAF operation's stability limits comprehensively. The primary objective of these tests was to identify specific disturbances that could potentially trigger unstable behavior in the process. This exploration is important for identifying information to be used in the subsequent closed-loop system experiments, where maintaining stability is paramount. So, we can test the closed loop under disturbances that can make the system unstable.

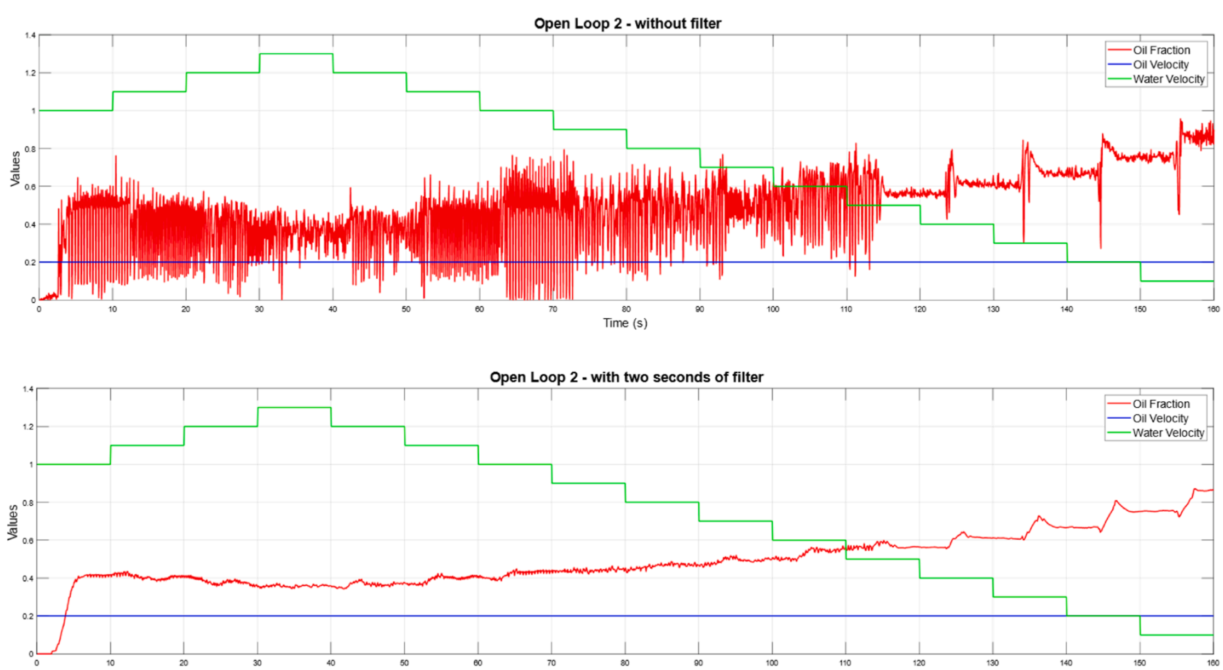

Fig. 6b. Open loop for oil velocity 0.2 m/s.

Fig. 7. Simulation $T_0 = 0\ s,\ oil\ velocity = 0\frac{m}{s}\ and\ water\ velocity = 0\frac{m}{s}$.

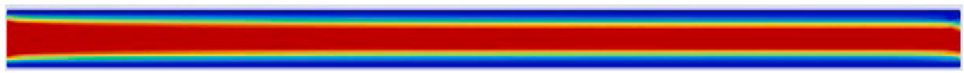

Fig. 8. Simulation $T = 10\ s,\ water\ velocity = 0.4\frac{m}{s}, oil\ velocity = 0.2\frac{m}{s},\ rate = 2$.

Fig. 9. Comparison between rate 2 and 1.5.

The first of these open-loop tests concentrated on manipulating water velocity while keeping oil velocity constant, treating the latter as a disturbance. This method provided insights into the effects of water flow variations on the system's stability. In the subsequent open loop test, the focus shifted to manipulating oil velocity, while keeping water velocity constant. Based on this second open-loop test, we identified the disturbance threshold that could push the system out of its stable zone and into a slug flow behavior. This latter specific oil velocity disturbances where then employed in the closed-loop control experiments to assess the controller's capability to stabilize the system under such challenging conditions.

3. Open loop results

To begin with, it is essential to recognize that there are countless combinations of oil and water velocities that can influence the flow pattern within the system. These variations can arise from factors such as pipe inclination, direction, diameter, and length. Consequently, to identify the region where the flow exhibits the greatest instability, a simulation was conducted, accompanied by a rendering of the specific moment, to gain a deeper understanding of the system's behavior.

In an operational process, the primary objective is typically to transport the maximum possible amount of material, which can sometimes push the system into potentially dangerous operating regions. To assess this, an open-loop test was conducted at varying speeds. Given the rapid dynamics of the oscillation phenomenon, 2 s moving average filter was applied to better capture and understand the system's behavior.

In Figs. 6a and 6b, the open-loop test is shown using oil velocities of 0.5 m/s and 0.2 m/s, changing the velocity of water in the scale of m/s.

As expected, the operation at a lower velocity resulted in increased instability, as the buoyancy effect becomes more pronounced under these conditions. This leads to oil stratification, disrupting the annular flow. Thus, a velocity for oil of 0.2 m/s was strategically chosen as the control point in a critical area, given its noticeable instability.

Following this, a shorter open-loop test was conducted to capture frames of specific regions and closely observe the phenomenon. The system was fully initialized with water, as shown in Fig. 7. The outlet pressure was considering the atmosphere pressure and the initial velocity of water and oil, that is $0\frac{m}{s}$ for water and oil to $T = To = 0\ s$.

After this initial condition, the experiments start with water velocity $= 0.4\frac{m}{s}$ and oil velocity $= 0.2\frac{m}{s}$ for $T = To + \Delta T$, where $\Delta T = 0.05\ s$. The state of the system after the first 10 s with such feed can be seen in Fig. 8. Considering the $Ratio = \frac{water\ velocity}{Oil\ velocity}$.

These first 10 s are sufficient for the system to reach the CAF with stability. After that, the simulations were conducted with a fixed oil velocity of 0.2 m/s, while varying the water injection velocity, effectively altering the water-to-oil ratio, which leads to CAF with distinct dynamical behaviors. These variations were initiated at 10 s to observe the system's response to changes in the injection conditions.

The first phenomenon to observe is that as we reduce the water injection speed to $0.3\frac{m}{s}$, there is a noticeable increase in the oil core in the pipe. This is illustrated in Fig. 9, which shows part of the pipe for the 2

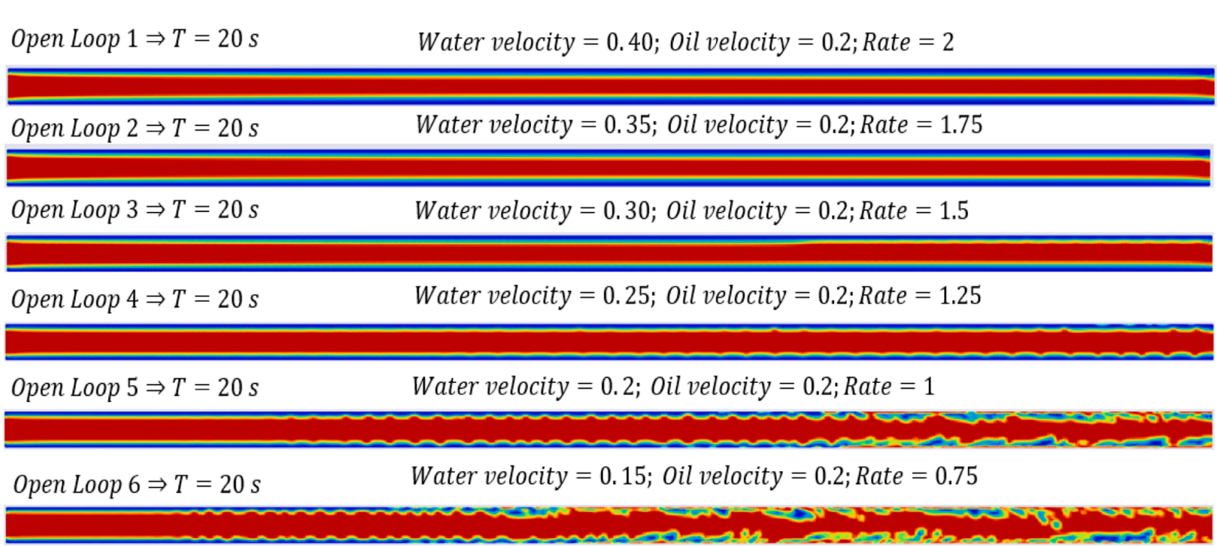

Fig. 10. Open loop I, simulation results of oil core with distinct water velocities.

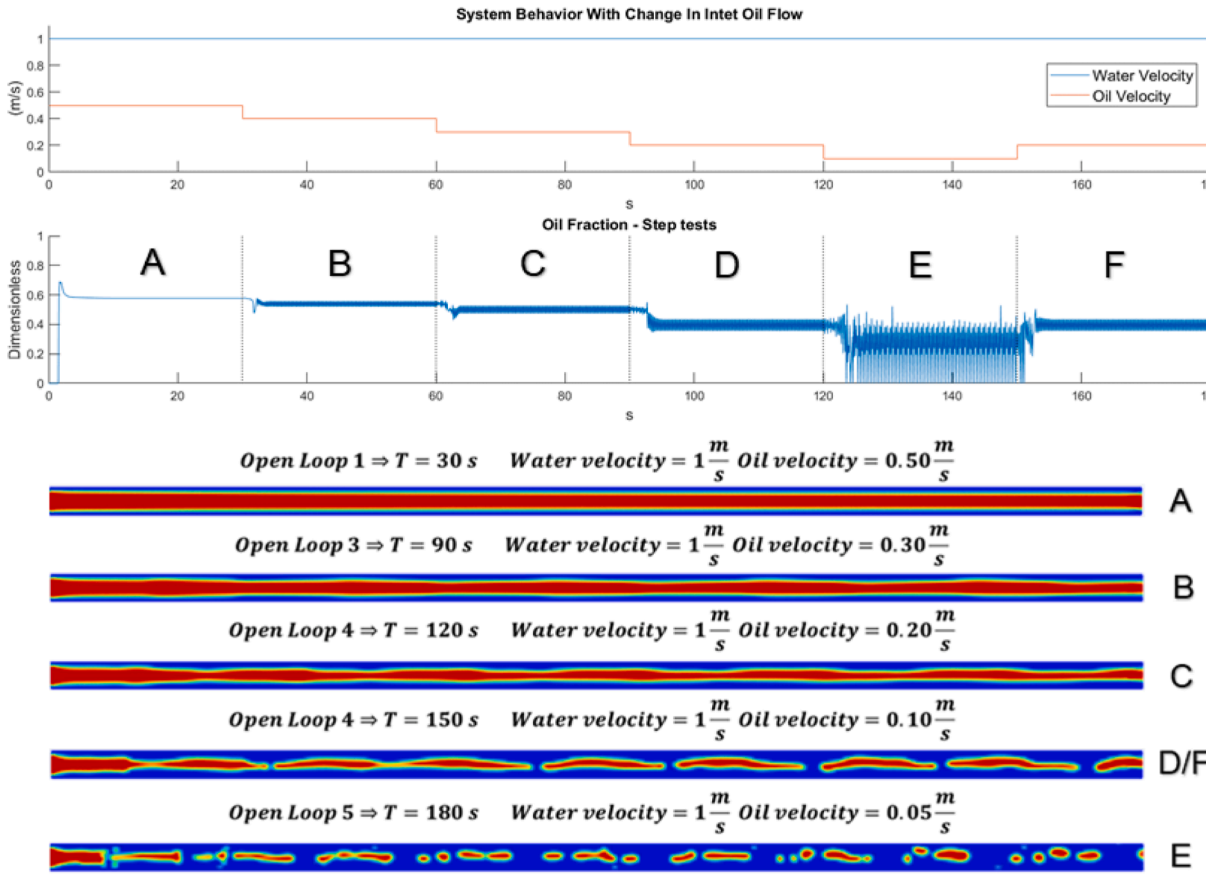

Fig. 11. Open loop II, simulation results.

and 1.5 rates. Note also that even with the flow presenting stable behavior, there are small oscillations occurring on the contact surface between the fluids.

The complete simulations are shown in Fig. 10, based on the initial state illustrated in Fig. 7. As the water velocity (the manipulated variable) changes, the oil fraction (the controlled variable) also changes, affecting the behavior of the oil core. It is important to observe how the modified injection boundary conditions impact the system's stability at the specified instant. Also note that the flow patterns with oil fraction around the rate 2, results in the oil fraction = 0.58 and show stable behavior along the entire pipeline. This indicates a desired operating point for the system.

Observe that as the speed is reduced, the impact of thrust becomes increasingly significant for the system. This results in the initial disturbances within the oil core becoming evident at a rate of 1.25 in Fig. 10.

When the rates reach 1 and 0.75, there is complete instability within the oil core at the center of the pipe. This occurs because as the water speed decreases substantially, its capacity to transport the oil along the horizontal axis is reduced. Consequently, the buoyancy vector becomes significant enough to generate vertical movement in the oil mass, eventually leading to encrustation within the pipe, as the oil is more viscous but less dense.

These results underscore a critical aspect: if the system lacks stabilizing properties, it can inadvertently lead the process towards unstable operation by the changes in oil and water velocities.

In the second open-loop test, the water velocity was considered constant and is considered that disturbs steps varies the oil velocity. The results can be seen in Fig. 11. Hence, through this test, one can dynamically understand the system's behaviors in the presence of disturbances. This approach allows for a comprehensive analysis of how the system responds to variations in oil velocity disturbances, providing valuable insights into its stability under operational changing conditions.

In Fig. 11, the transition from annular flow to slug flow is visible. In parallel, it is possible to follow the variation in the oil fraction signal. As the pattern transition progresses, it is possible to notice the presence of greater oscillations in the slug flow.

Note in the time trends that the flow regime in the annular pattern shown in the time windows "A, B, C" behaves as approximately as a first-order system, stabilizing around a value after the input step. In addition, as the flow regime changes to the slug pattern in the "E" time window, the system changes its behavior to a second-order system with imaginary poles, presenting an oscillatory steady state. The system acts in an intermediate way between these previous patterns in the time windows "D" and "F" when the system changes because the process non-linearity and small oscillations start.

Maintaining the integrity of the oil core is crucial for stable and efficient pipeline operation and controlling injection speeds is essential to achieve this. To prevent such complications, monitoring and managing the injection velocities carefully is important, ensuring a stable and efficient flow of oil within the pipeline. However, dealing with the different flow patterns and their contrasting dynamical characteristics is a control challenge, which in this context is usually neglected.

4. Closed loop results

4.1. Structure of control

A critical element of this system is the Oil Fraction Measurement unit, tasked with the continuous monitoring of the oil fraction. To prevent minor oscillations from disrupting the closed-loop system and potentially causing instability, this measurement is relayed to the

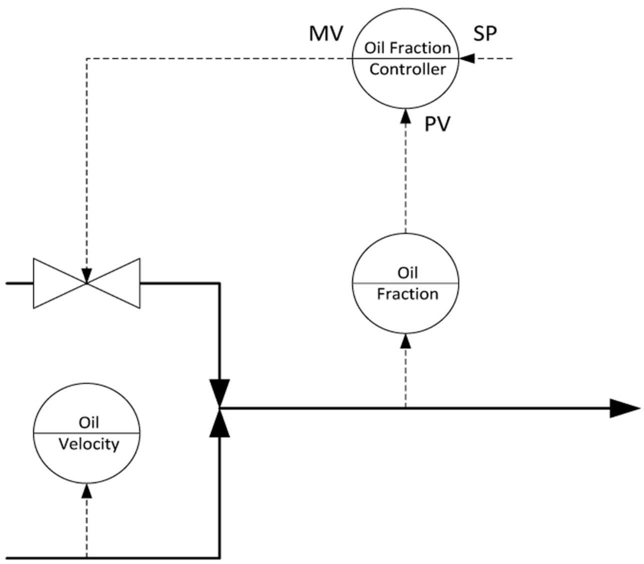

Fig. 12. Proposed stabilizing control structure.

controller through a moving average filter of 2 s. In a real physical process, to measure the oil fraction in one multiphase system, normally one could use Coriolis flow meters and ultrasonic-based sensors (Corneliussen et al., 2005). This control approach ensures real-time adjustments are made to preserve the desired oil fraction. Additionally, the Oil Velocity Measurement module indicates the flow velocity, offering valuable insights into potential disturbances that might destabilize the oil core. Such disturbances could arise from fluctuating injection speeds. Within this operational framework, the system is expected to adeptly counter the effects of varying injection speeds, thereby ensuring a consistent oil flow within the pipeline. This is achieved by maintaining the oil fraction at the predetermined setpoint, thereby enhancing the overall stability and efficiency of the system.

The proposed control structure is presented in Fig. 12. The control system presents a closed-loop feedback mechanism for oil flow stabilization within a pipeline. Central to this system is the Oil Fraction Controller, which adjusts the Manipulated Variable (MV), the water velocity, based on the discrepancy between the Setpoint (SP) and the Process Variable (PV), the latter being the real-time measurement of the oil fraction.

In the closed loop tests, the system will start with an initial water velocity of 0.7 m/s and the oil velocity set at 0.3 m/s, after this the value will be reduced as disturbance to 0.25 m/s and 0.2 m/s. This value was chosen because, as seen in Figs. 11 and Fig. 10, is expected that this configuration will reproduce the annular flow of the core.

Subsequently, the oil velocity will be perturbed decremental until reaching values corresponding to zone C in Fig. 10, where it is possible to see where the oscillation behavior starts to be stronger. This procedure will comprehensively evaluate the effectiveness of the control strategy in stabilizing the system under these specific conditions.

4.2. Tunning of system

Considering all the knowledge acquired during the open-loop tests 1 and 2, it was identified that regions near an oil velocity of 0.2 tend to destabilize the system, altering the behavior of the core annular flow. A transfer function identification was performed near this control region, which is of particular interest to us to prevent disturbances from altering the flow $G(s) = e^{-425s}. - \frac{0.7288}{s+1.558}$ pattern.

Considering the transfer function obtained, as shown in Fig. 13, it is evident that the delay, 4.25 s, is significantly larger than the system's time constant, 0.64 s. This indicates that the system's dynamics are predominantly influenced by the dead time, classifying it as a dead-time-dominated system. In such a scenario, it is appropriate to approximate the model as a Pure Time Delay system, disregarding the time constant relative to the dead time, to simplify the analysis and controller design.

Since this system can be approximated as a pure time delay, an integrator-only controller can be employed, as described by Eq. (1) (Skogestad, 2003).

$$K_I = \frac{1}{k(\tau_c + \theta)} \tag{1}$$

Where K_I is the integral gain of the controller, k is the system gain, τ_c is the desired closed loop response time and θ is the dead time or delay (Skogestad, 2003). Considering that the system is not linear, Figs. 6a and 6b, values o k can be different, for this was calculated different values of

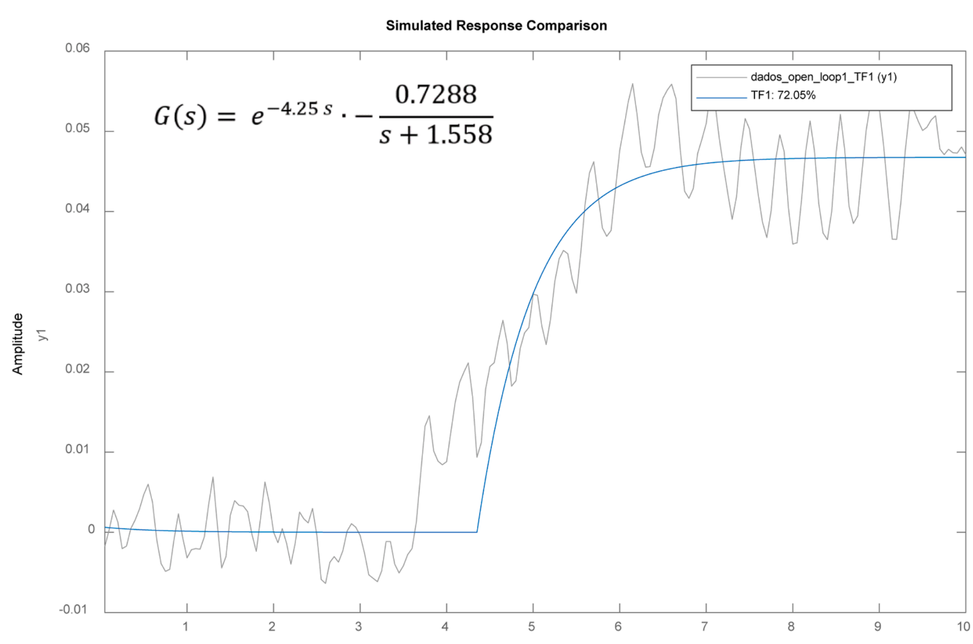

Fig. 13. Identification of transfer function.

Table 2
Values of K_I.

Description	k	$K_I\left(\frac{m}{s^2}\right)$
Under of lowest gain	−0.25	−0.245
Lowest gain	−0.51	−0.122
Between lowest gain and mean gain	−0.68	−0.090
Mean gain	−0.78	−0.079
Highest gain	−1.06	−0.058

K_I considering $\tau_c = 8\ s8$ and $\theta = 8\ s8$, Table 2.

A smaller proportional gain K results in a slower or less sensitive response to errors between the set point and the system output. To compensate for this reduced sensitivity, the integral K_I must be increased.

A controller is employed across various simulation experiments to manage the dynamics of the oil fraction within the cross-section in a closed-loop system. The controller aims to prevent the system from steering through the diverse dynamics of each flow regime pattern, as detailed in the open-loop results section.

This approach improves system stability and expands the operational range, allowing for the automatic rejection of disturbances in oil velocity. By doing so, the system can be operated in regions initially deemed unstable or prone to slug behavior. This enhancement not only broadens the operational capabilities but also ensures more reliable and efficient performance in previously challenging or risky conditions. All results of simulation can be seen in Fig. 14. Additionally, a set point result of 0.58 was rendered for system visualization, Fig. 15.

The first important observation is that the system in question exhibits nonlinear characteristics. This means that the system's responses vary differently depending on the region of operation and the K_i gain used. A common aspect of nonlinear systems is that the same gain value can result in different responses in different operating regions, a phenomenon that is evident in Fig. 14.

When the system is close to the set point (0.58), the response tends to be more stable and controllable with certain K_i values. However, when the system deviates from the set point due to disturbances (like in the 80 s and 160 s), the response can vary significantly, especially with higher K_i values. This behavior highlights the complexity of controlling nonlinear systems, where the same K_i gain can produce different effects in different parts of the control curve.

Another issue that becomes clear from the analysis of the graphs is the overshoot that appears when K_i values are higher. As K_i increases, the controller reacts more aggressively to quickly reach the set point. While this aggressiveness may reduce stabilization time in an ideal scenario, it also increases the overshoot.

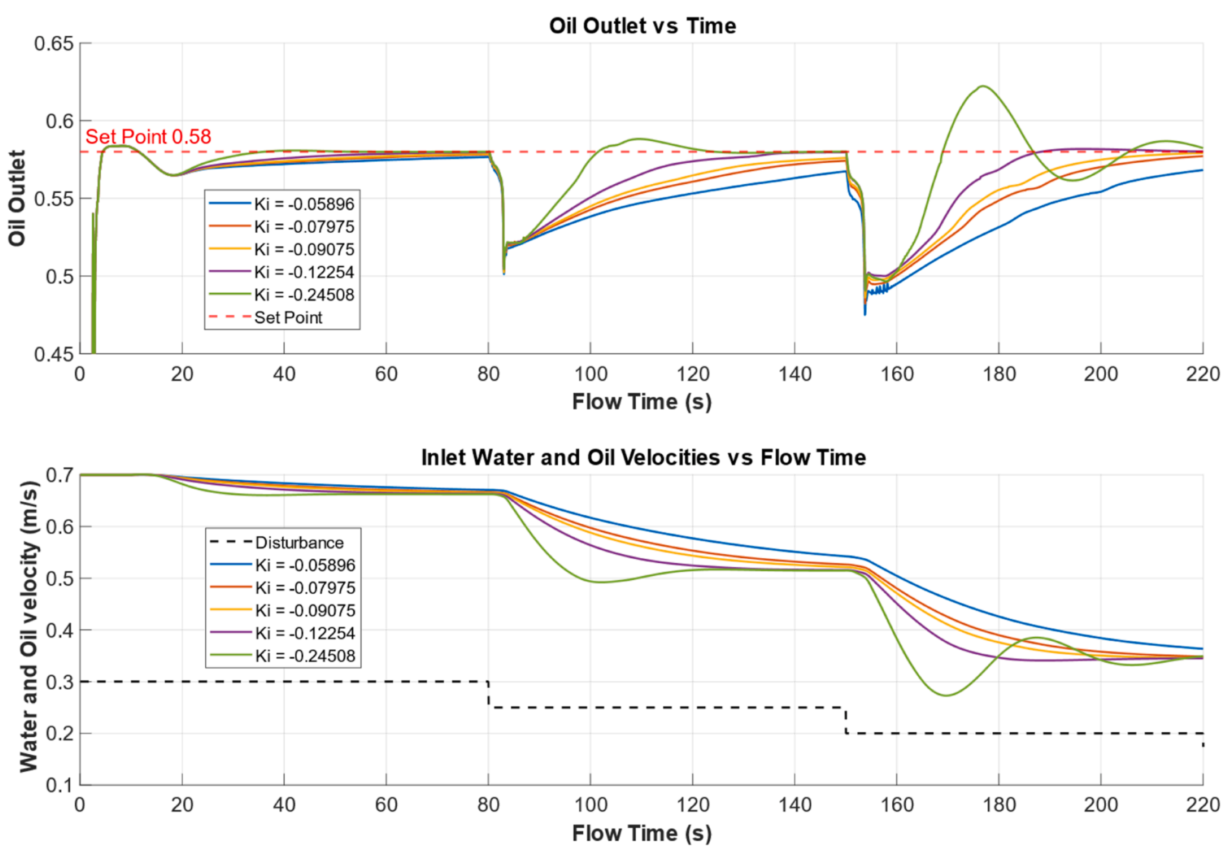

Fig. 14. Results of closer loop.

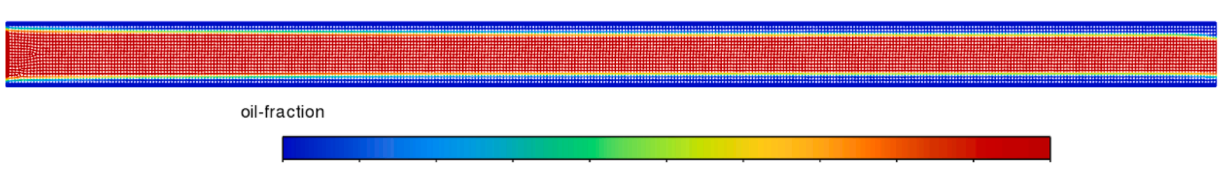

Fig. 15. System visualization at oil fraction 0.58.

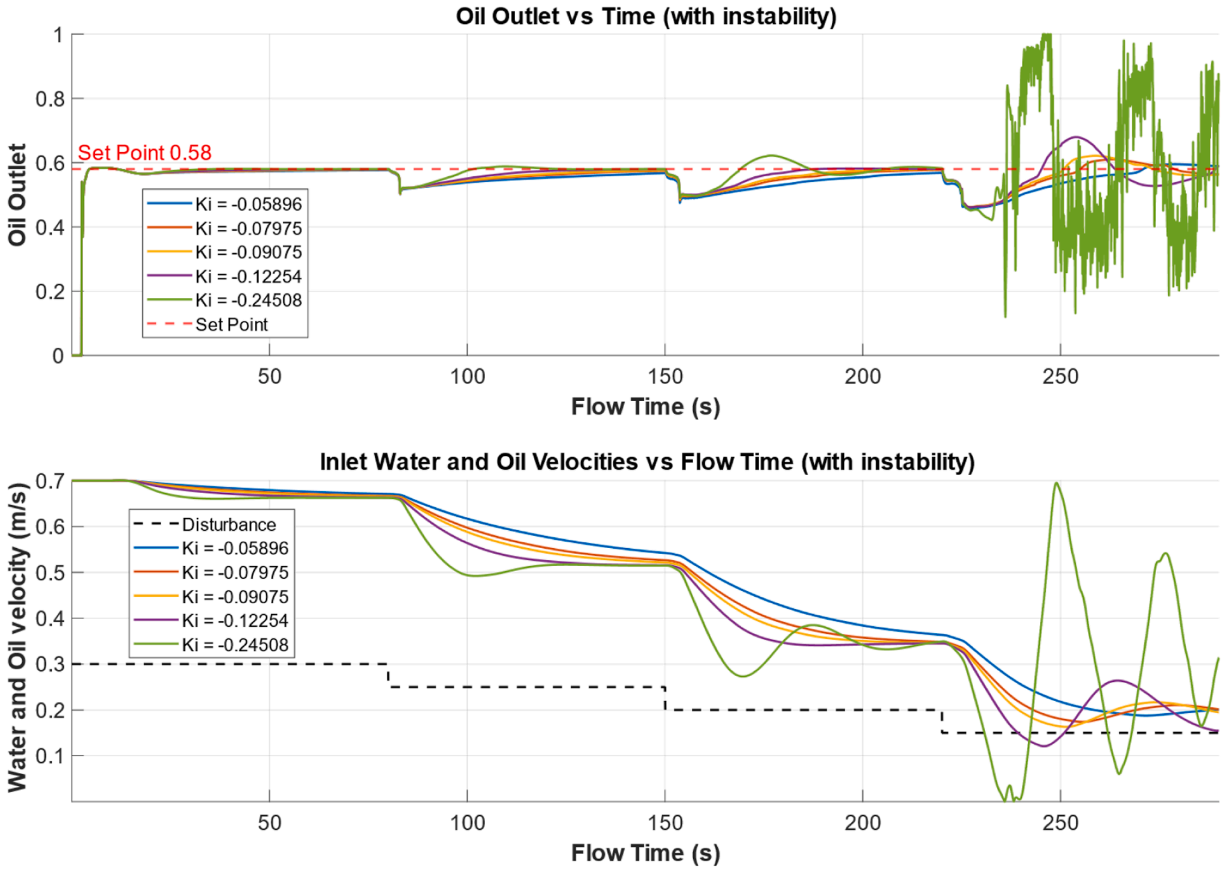

Fig. 16. Results of closer loop (with instability).

Overshot is not necessarily harmful in linear or well-behaved systems, but in a nonlinear system, it can lead to undesirable consequences, such as continuous oscillations or even instability. This occurs because, in a nonlinear system, the return to the set point after an overshoot can be unpredictable and vary drastically depending on the state of the system at that moment as seen in Fig. 16.

In the case of higher K_i gains (as seen with $K_i = -0.24508$), the system begins to oscillate significantly, and the controller ends up "overworking", generating a response that is neither efficient nor stable under more severe disturbances, leading to the moment where the water velocity reaches 0, completely destroying the water lubricating layer in the high viscosity oil, leading to a large increase in pumping energy due to the complete clogging of the pipeline by oil.

The choice of Ki values and control strategy depends directly on the operating conditions and the type of disturbances encountered. In a plant with low disturbance oscillation (such as constant oil velocity or minimal variations), it is possible to apply more aggressive Ki values to reach the set point faster, as the risk of overshot and instability is reduced. Using higher Ki values can be a valid strategy in this type of scenario to increase productivity and minimize stabilization time.

5. Conclusions

The Core Annular Flow is important in the oil and gas industry, especially when transporting viscous fluids like heavy oil. However, maintaining the stability of CAF over large distances can be challenging, with issues such as geometric variations, changes in the direction of the pipeline flow, and emulsion formation possibly destabilizing the flow.

Applying control techniques has shown to be a promising solution to overcome these challenges and improve the overall performance of oil and gas transportation processes. However, no reports were found in the literature proposing control structures for CAF flow stabilization and control. This research used the Computational Fluid Dynamics (CFD) method to simulate a CAF system and subsequently create I control strategy to manage this process. Furthermore, open-loop and closed-loop tests were carried out to understand whether the found parameters were sufficient to control the system quickly and effectively.

The results indicate that the integrity of the oil core is fundamental for efficient pipeline operation. Introducing the I controller has proven particularly effective in reducing oscillations around the setpoint and preventing the system from trending toward unstable regions in the presence of disturbances. This is a notable advancement, especially when compared to the open-loop scenarios where the system showed a greater propensity for instability under similar conditions. Furthermore, the fine-tuning of the I controller, with a specific focus on the SIMC-PID rules, has resulted in a smoother closed-loop response. This refinement has not only enhanced the system's ability to closely follow the setpoint but has also allowed for stable operation in conditions that were previously challenging or unstable.

Our findings confirm that the nonlinearity of the system plays a significant role in determining the effectiveness of different K_i values. As shown in the results, the response of the controlled variable (oil outlet) varies in different operating regions, highlighting the complexity of nonlinear systems. Specifically, the use of higher K_i values lead to overshoot, which can result in system instability, particularly in scenarios involving significant disturbances. This indicates that while aggressive K_i values can reduce the time to reach the set point, they also introduce oscillations that may compromise system stability.

The results demonstrate that the I controller, when appropriately tuned, can stabilize the CAF system in a wide range of conditions. However, the trade-off between response speed and stability must be carefully managed. This research paves the way for new strategies of control to turn the operation more stable, safety and profitable in CAF operations.

CRediT authorship contribution statement

Patrick Lima: Writing – review & editing, Writing – original draft, Software, Methodology, Investigation, Conceptualization. **Erbet Costa:** Writing – review & editing, Writing – original draft, Visualization, Formal analysis. **Teófilo Paiva Guimarães Mendes:** Writing – review & editing, Writing – original draft, Visualization, Formal analysis. **Leizer Schnitman:** Writing – review & editing, Writing – original draft, Formal analysis. **Sigurd Skogestad:** Writing – review & editing, Writing – original draft, Methodology, Formal analysis, Conceptualization. **Idelfonso Nogueira:** Writing – review & editing, Writing – original draft, Supervision, Methodology, Formal analysis, Conceptualization.

Declaration of competing interest

The authors declare that they have no known competing financial interests or personal relationships that could have appeared to influence the work reported in this paper.

Data availability

The authors are unable or have chosen not to specify which data has been used.

References

ANSYS Inc. (2009). ANSYS Fluent Theory Guide, Release 12.
Bensakhria, A., Peysson, Y., Antonini, G., 2004. Experimental study of the pipeline lubrication for heavy oil transport. Oil & Gas Sci. Technol. 59 (5), 523–533.
Brackbill, J.U., Kothe, D.B., Zemach, C., 1992. A continuum method for modeling surface tension. J. Comput. Phys. 100, 335–354.
Corneliussen, S., et al. (2005). Handbook of Multiphase Flow Metering. The Norwegian Society for Oil and Gas Measurement (NFOGM) and The Norwegian Society of Chartered Technical and Scientific Professionals (Tekna).
Dianita, D.S., Siregar, M.R., Kurnia, J.C., 2021. CFD simulation and statistical experimental design analysis of core annular flow in T-junction and Y-junction for oil-water system. J. Pet. Sci. Eng. 205, 108874.
Erni, P., Fischer, P., Heyer, P., Windhab, E.J., Kusnezov, V., Läuger, J., 2004. Rheology of gas/liquid and liquid/liquid interfaces with aqueous and biopolymer subphases. In: Progress in Colloid and Polymer Science, 129. Springer, Berlin, Heidelberg.
Ghosh, S., Das, G., Das, P.K., 2010. Simulation of core annular downflow through CFD-A comprehensive study. Chem. Eng. Process. 49 (11), 1222–1228. https://doi.org/10.1016/j.cep.2010.09.007.
Jahanshahi, E., Skogestad, S., 2013. Closed-loop model identification and PID/PI tuning for robust anti-slug control. In: IFAC Proceedings Volumes (IFAC-PapersOnline), 10, pp. 233–240. https://doi.org/10.3182/20131218-3-IN-2045.00009.
Jahanshahi, E., Skogestad, S., Hansen, H., 2012. Control structure design for stabilizing unstable gas-lift oil wells. In: IFAC Proceedings Volumes (IFAC-PapersOnline), (PART 1), pp. 93–100. https://doi.org/10.3182/20120710-4-SG-2026.00110.
Jiang, F., Wang, Y., Ou, J., Chen, C., 2014. Numerical simulation of oil-water core annular flow in a U-bend based on the eulerian model. Chem. Eng. Technol. 37 (4), 659–666. https://doi.org/10.1002/ceat.201300809.
Joseph, D.D., Bai, R., Chen, K.P., Renardy, Y.Y., 1997. Core-annular flows. Annu Rev Fluid Mech 29, 65–90.
Rosa, E.S. (2012). Escoamento multifásico isotérmico: modelos de multifluidos e de mistura.
Salager, J.-L., Bullon, J., Pizzino, A., Rondón-González, M., Tolosa, L., 2010. Emulsion formulation engineering for the practitioner. In: Encyclopedia of Surface and Colloid Science, pp. 1–6.
Sivertsen, E., Storkaas, E., 2010. Mini-slug flow dynamics and control in microchannels. Chem. Eng. Res. Des.
Skogestad, S., 2003. Simple analytic rules for model reduction and PID controller tuning. J. Process Control 13 (4), 291–309.
Storkaas, E., 2002. Analysis of fluid dynamics in pipeline systems. AlChE J.
Storkaas, E., 2005a. Control applications in pipeline systems. In: IFAC Proceedings Volumes.
Storkaas, E., 2005b. PhD Thesis on Slug Flow Dynamics and Control. NTNU.
Storkaas, E., 2007. Controllability of Slug Flows in Pipelines. Chemical Engineering Progress.
Tripathi, S., Tabor, R.F., Singh, R., Bhattacharya, A., 2017. Characterization of interfacial waves and pressure drop in horizontal oil-water core-annular flows. Phys. Fluids 29 (8). https://doi.org/10.1063/1.4998428.
Versteeg, H.K., Malalasekera, W., 2007. An Introduction to Computational Fluid Dynamics: The Finite Volume Method, 2nd Edition. Pearson.
Xie, B., Jiang, F., Lin, H., Zhang, M., Gui, Z., Xiang, J., 2023. Review of core annular flow. Energies 16 (3), 1496. https://doi.org/10.3390/en16031496.